

Reversal of liver cancer-associated stellate cell-induced stem-like characteristics in SMMC-7721 cells by 8-bromo-7-methoxychrysin via inhibiting STAT3 activation

YINGHONG CUI*, SHUWEN SUN*, KAIQUN REN, MEIFANG QUAN,
ZHENWEI SONG, HUI ZOU, DUO LI and JIANGUO CAO

Department of Pharmaceutical Science, Medical College, Hunan Normal University, Changsha, Hunan 410013, P.R. China

Received November 24, 2015; Accepted December 27, 2015

DOI: 10.3892/or.2016.4637

Abstract. Hepatic stellate cells (HSCs) that are activated by human hepatocellular carcinoma (HCC) cells secrete a variety of cytokines, which are the main component of the HCC microenvironment. We aimed to determine whether 8-bromo-7-methoxychrysin (BrMC) could interfere in cross-talk of the human hepatic stellate cell line LX-2 and liver cancer stem-like cells (LCSLCs) to inhibit the characteristics of LCSLCs endowed with the capacity of sustaining human hepatocellular carcinoma (HCC) self-renewal and progression, and to identify its potential mechanism of action. We found that the levels of fibroblast activation protein (FAP) were augmented in LX-2 cells treated with the conditioned medium of LCSLCs (LCSLC-CM) compared to those cultured with routine medium, indicating that the LCSLC-CM can activate LX-2 cells to become liver cancer-associated stellate cells (LCAHSCs). Furthermore, sphere forming capability of SMMC-7721 cells was enhanced and stem cell-related protein expression was significantly increased following treatment with the conditioned medium of LCAHSCs (LCAHSC-CM). Moreover, the level of p-STAT3 was increased in LX-2 cells treated with LCSLC-CM and BrMC reduced expression of p-STAT3. Combination of BrMC and the selective inhibitor of STAT3 cucurbitacin I (JSI-124) synergistically suppressed the LCSLC characteristics in SMMC-7721 cells. Collectively, our data showed that BrMC inhibited the interaction between LX-2 cells and HCC-derived CSCs, and did so potentially through modulation of the STAT3 pathway. Future thera-

peutic strategies employing anti-CSC therapy should confirm the potential of cucurbitacin I (JSI-124) and BrMC as potent therapeutic agents.

Introduction

The fifth most common cancer globally is human hepatocellular carcinoma (HCC), and in the context of cancer-related mortality HCC ranks third as one of the leading causes (1,2). Moreover, traditional therapy remains disappointing. It is believed that HCC is sustained by liver cancer stem cells (LCSCs), which constitute a relatively small frequency of cells, and they do so through their ability to propagate highly heterogeneous progeny, multi-drug resistance to chemotherapeutic agents and a high capacity for cellular proliferation (3). A number of studies have suggested that LCSCs can be identified by several cell surface antigens including CD133, CD44, and ALDH1 (4-6). Furthermore, CD133⁺, CD44⁺ and ALDH1⁺ cells that are isolated from HCC cells display an enhanced capacity for malignant transformation *in vivo*. These studies indicate LCSCs as the basis of HCC. However, emerging evidence shows that cancer onset and progression was not only determined by tumor cells but was also affected by the local microenvironment (7,8).

It has been reported that almost 80% of hepatocellular carcinoma (HCC) resulted from chronic hepatitis and cirrhosis caused by inflammation and fibrosis (9). Hepatic stellate cells (HSCs), which are the main liver stromal cells, can transform into a myofibroblast-like phenotype from a quiescent state during chronic liver injury (10,11). An important cellular source of hepatic-derived cytokines (e.g., TGF- β , PDGF, HGF, FGF, and VEGF) is secreted by HSCs that constitute the main component of the local liver cancer microenvironment. Additionally, HSC activation might play an important role in inflammation and fibrosis, even during tumor metastasis (9). It has been shown recently that malignant transformation in HSC is critical in reprogramming cells that transform the physiologically normal vitamin-A storage capacity of HSC to a remodeled extracellular matrix phenotype (11), which then provides a tumorigenic environment that is compatible for HCC. Additionally, studies have shown that cross-talk of hepatocytes and HSC can generate a permissive inflammatory

Correspondence to: Dr Jianguo Cao, Department of Pharmaceutical Science, Medical College, Hunan Normal University, Changsha, Hunan 410013, P.R. China
E-mail: caojianguo2005@126.com

*Contributed equally

Key words: hepatocellular carcinoma, hepatic stellate cell, liver cancer stem cells, liver cancer-associated stellate cell, 8-bromo-7-methoxychrysin, STAT3, SMMC-7721 cells

microenvironment to promote HCC development (12), and the interaction of hepatocytes and HSCs leads to tumor metastasis, proliferation and chemotherapy resistance (13). However, whether LCSCs activate HSC in a way that promotes HCC progression remains to be fully explored.

Signal transducer and activator of transcription-3 (STAT3), a transcription factor for cytokine signaling, is constitutively activated in numerous cancer types, including prostate cancer, breast cancer, leukemia, brain tumors, and lung cancer (14-18). Niu *et al* reported that STAT3 mutations induced cellular transformation and tumor formation *in vivo* and that activation of STAT3 signaling further inhibited p53 transcriptional activity, fulfilling the definition of an oncogene (19). In addition, it is reported that activated STAT3 could promote LCSCs (20). Moreover, activation of STAT3 in hepatic stellate cells promoted their survival and proliferation, thereby contributing to liver fibrogenesis (21,22). However, the mechanism of the STAT3 signaling pathways to interrupt cross-talk of LSCs and HSC and the possible therapeutic targets involved in HCC need further investigation.

Cucurbitacin I (JSI-124) is a cell permeable, triterpenoid compound that was shown to specifically suppress tyrosine phosphorylation of STAT3 (23). In the current study, we hypothesized that JSI-124 would be useful to block cross-talk of LCSCs and HSC by inhibiting activation of STAT3.

Chrysin (5,7-dihydroxyflavone, ChR), a natural widely distributed flavonoid, has been shown to possess promising effects on the inhibition of proliferation and induction of apoptosis in a variety of cancer cells (24,25). By using a STAT3-specific inhibitor, JSI-124, Lirdpramongkol *et al* showed that ChR overcame TRAIL resistance of cancer cells through inhibiting STAT3 phosphorylation (26). Furthermore, Lin *et al* reported that ChR suppresses IL-6-induced angiogenesis through modulation of the STAT3 signaling pathway (27). In a previous study, we succeeded in synthesizing 8-bromo-7-methoxychrysin (BrMC) based of the lead compound ChR (28). Compared to ChR, BrMC has stronger effects of inhibition of proliferation and induction of apoptosis on colon cancer cell line HT-29 and gastric cancer cell line SGC-7901 (28,29). As previously described, BrMC can inhibit the proliferative activity of glioma stem-like cells, and target to inhibit the characteristic of LCSCs (30,31). Thus, our aim was to analyze if BrMC can affect cross-talk of liver cancer stem cells and HSC to reduce the activation of HSC and inhibit the properties of LSCs by suppressing STAT3.

Materials and methods

Reagents. Dulbecco's modified Eagle's medium (DMEM) and DMEM/F12 medium, Trypsin-EDTA, FBS and Penicillin-streptomycin were from Gibco (Grand Island, NY, USA). All cell culture ware was from Corning Life Sciences (New York, NY, USA). Monoclonal anti- α -SMA-Cy3 antibody was obtained from Sigma-Aldrich (St. Louis, MO, USA). Polyclonal anti-FAP- α , polyclonal anti-E-cadherin, polyclonal anti-N-cadherin, monoclonal anti-CD33, monoclonal anti-CD44, monoclonal anti-stat3, and polyclonal anti-ALDH1 antibody were obtained from Abcam (Hong Kong, China). The STAT3 inhibitor, JSI-124, was obtained from Sigma-Aldrich, and was

prepared by dissolving in DMSO to a stock concentration of 100 μ mol/l. JSI-124 was additionally diluted in culture medium to required final concentrations immediately prior to use. BrMC was synthesized as previously described (28). All other experimental reagents used in this study were obtained from Sigma-Aldrich, unless indicated otherwise in the text.

Cell culture and sphere formation assay. The Chinese Academy of Sciences (Shanghai, China) provided the human liver cancer SMMC-7721 cell line. The human immortalized HSCs (LX-2) was obtained from Bogu Biotechnology Co., Ltd. (Shanghai, China). Cells were routinely passaged in complete DMEM that was supplemented with 10% fetal bovine serum (FBS), and antibiotics. Cell cultures were incubated at 37°C in an atmosphere of 5% CO₂ in air.

Suspensions of single-cells were seeded into ultra low attachment 6-well plates (Corning Life Sciences) at a density of 3,000 cells/ml in stem cell-conditioned medium. Culture suspensions were passaged every five days when spheroid diameters were at least 50 μ m. Colonies were then scored under ten independent fields of view by light microscopy (Olympus, Tokyo, Japan). The efficiency of sphere formation was calculated by dividing the total sphere number that formed by the number of the total viable cells that were seeded multiplied by one hundred.

Preparation of conditioned medium from LSCs and LCAHSCs. To prepare LSC-CM, suspension culture and stem cell-conditioned medium amplification of LSCs was performed using ultra low-adhesion 6-well plates. Spent culture media was removed 24 h later, and this was filtered (0.22 μ m) and stored at -80°C until further use.

LX-2 cells were cultured with LSC-CM for 24 h, washed with PBS and serum-free DMEM, respectively, and incubated with serum-free DMEM for 24 h. Then the culture media was collected and centrifuged at 3000 rpm for 5 min, followed by filtering (0.22 μ m) as LCAHSC-CM and stored at -80°C for further use.

Immunofluorescence. LX-2 cells were cultured on coverslips, washed with PBS, fixed in 4% paraformaldehyde, following which, 0.1% triton X-100 for 4 min was used to permeabilize the cells. Next, monoclonal anti- α -SMA-Cy3 or polyclonal anti-FAP- α antibody was added for 45 min or 1 h at 37°C in the dark. Later, Alexa Fluor 488 anti-rabbit (Molecular Probes, 1:500, 1 h, RT) and DAPI [1:100, 10 min, room temperature (RT)] were incubated with the coverslips, which were then mounted for visualization and quantification. Images were collected by fluorescence microscopy (Olympus).

Western immunoblot analysis. Previously described procedures were used for preparing whole cell lysates and the western immunoblot procedure (32). The primary antibodies used in this procedure were monoclonal anti- α -SMA antibody, polyclonal anti-FAP- α , polyclonal anti-E-cadherin, polyclonal anti-N-cadherin, monoclonal anti-CD33, monoclonal anti-CD44, monoclonal anti-stat3, and polyclonal anti-ALDH1. In addition, internal loading of protein was controlled by detecting the expression of β -actin. Immunoblots were then visualized by chemiluminescent substrate (ECL; Amersham, Arlington

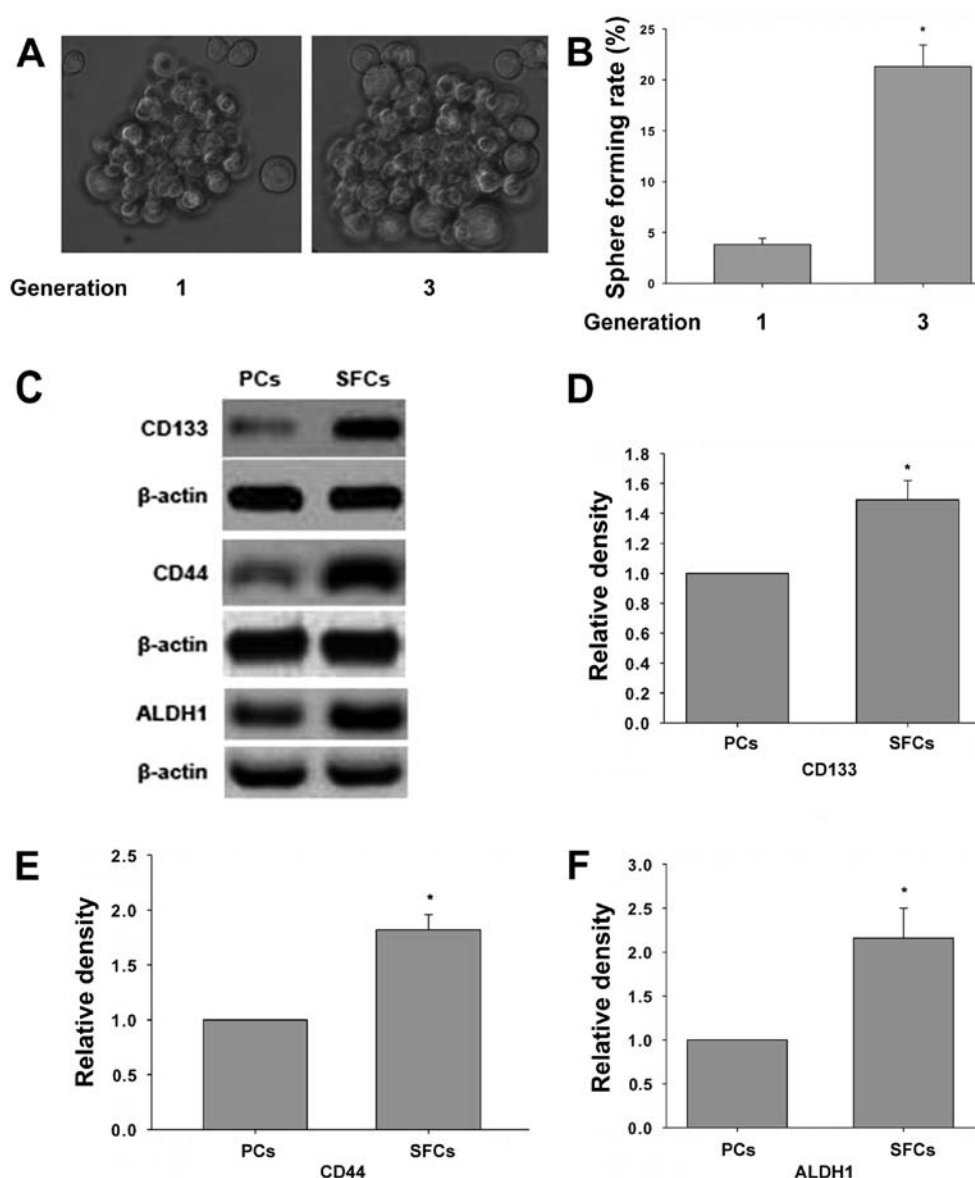


Figure 1. Increased expression of markers of stem cells and enhanced capability of sphere forming in sphere forming cells. (A) Representative images of the parental cells (left) and the third generation of sphere forming cells (right). (B) Sphere forming rate was calculated by counting the number of sphere forming cells (* $P < 0.05$). (C) Western blot expression of CD133, CD44 and ALDH1 in the parental cells and the third generation of sphere forming cells. Densitometry analysis to quantify the expression of CD133 (D), CD44 (E) and ALDH1 (F) protein, respectively (* $P < 0.05$).

Heights, IL, USA). The autoradiographed images were scanned to permit semi-quantitative densitometric analysis using UN-SCAN-IT software program (Silk Scientific).

Statistical analyses. Representative data described in this report are the product of at least three independent observations, unless otherwise indicated. The data were analyzed using analysis of variance followed by Dunnett's test for pairwise comparison. An asterisk indicates that the experimental values were significantly different from values at an α value of $P < 0.05$.

Results

Characteristics of liver cancer stem-like cells derived from SMMC-7721 cells. To investigate whether the third generation sphere forming cells (SFCs) of SMMC-7721 cell line possess

properties of liver cancer stem-like cells (LCSLCs), sphere formation assay was performed. Furthermore, the level of CD133, CD44, ALDH1 expression, which are known as markers of stem cells, were determined. Consistent with a previous study (30,31), the third generation of SMMC-7721 SFCs have stronger capability of proliferation and its sphere forming rate increases compared to parental cells (Fig. 1A and B). In addition, the expression of CD133, CD44, and ALDH1 is elevated in the third generation of SFCs compared to parental cells (Fig. 1C). These results indicated that the third generation SMMC-7721 SFCs have properties of LCSLCs.

Generation of liver cancer associated-stellate cells derived from human hepatic stellate cell line LX-2. Human hepatic stellate cell line LX-2 was exposed to conditioned medium from liver cancer stem-like cells (LCSLC-CM) for 24 h to generate liver cancer associated-hepatic stellate cells

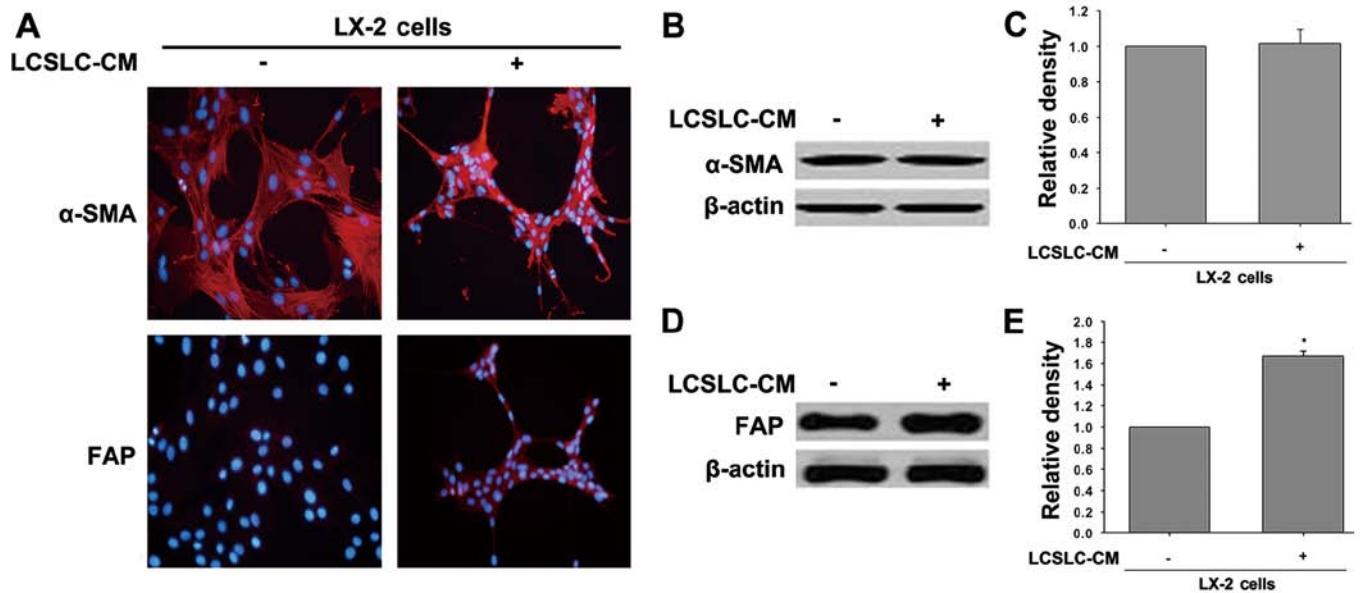


Figure 2. LX-2 cells are activated by LCSLC-CM. (A) Representative immunofluorescence images showing α -SMA and FAP expression, previously exposed to LCSLC-CM for 24 h, using serum-free medium as a control. Western blot expression of α -SMA (B) and FAP protein (D). To control for equal loading of protein samples, we used β -actin expression. (C and E) Densitometry analysis to quantify the expression of α -SMA and FAP protein (* P <0.05).

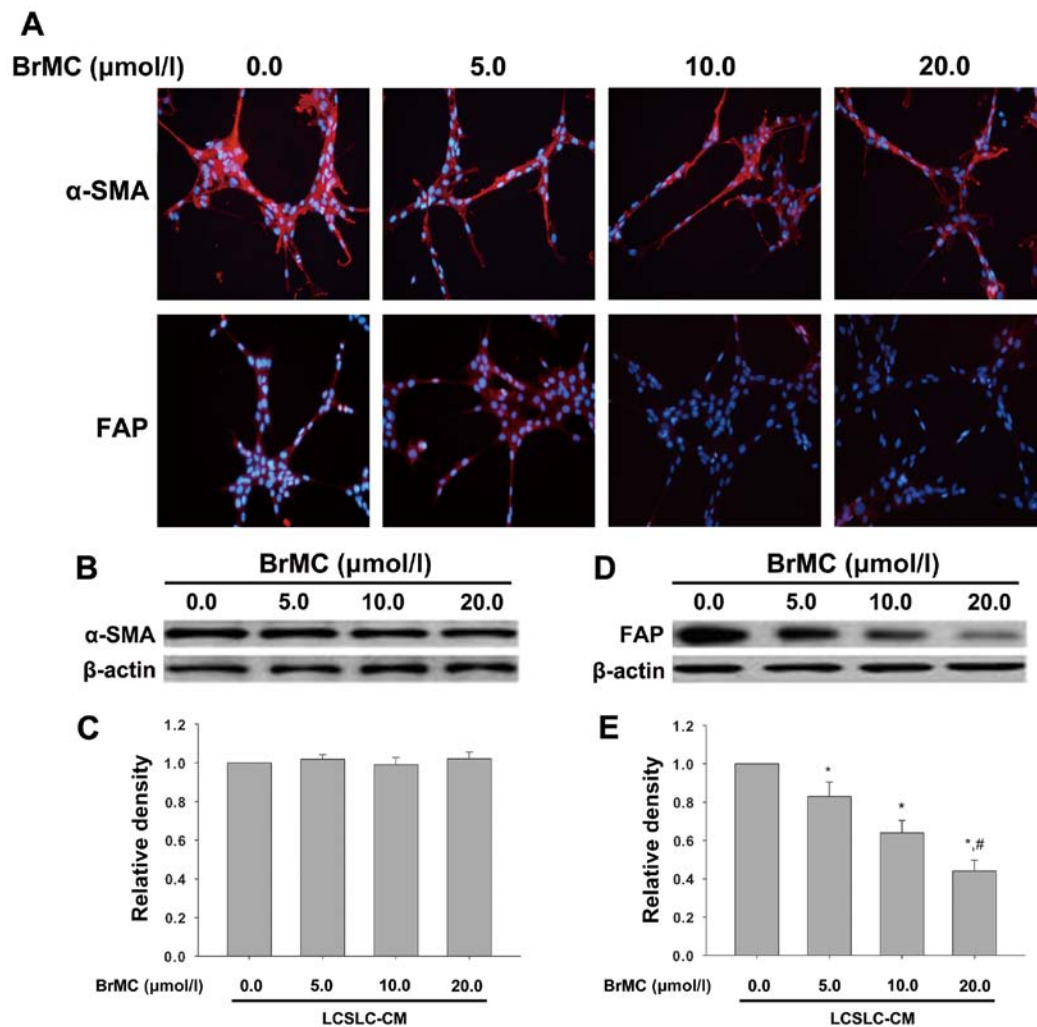


Figure 3. LCSLC-CM treated with BrMC reduces pathologically activated LX-2 cells. (A) Treated with LCSLC-CM containing different concentrations of BrMC (0.0, 5.0, 10.0, 20.0 μ mol/l), representative images of the expression levels of both α -SMA and FAP in LX-2 cells are shown. Western blot of the expression of α -SMA (B) and FAP (D) in LX-2 cells, and β -actin used as loading control. Densitometry analysis to quantify the expression of α -SMA (C) and FAP (E) protein, respectively (* P <0.05).

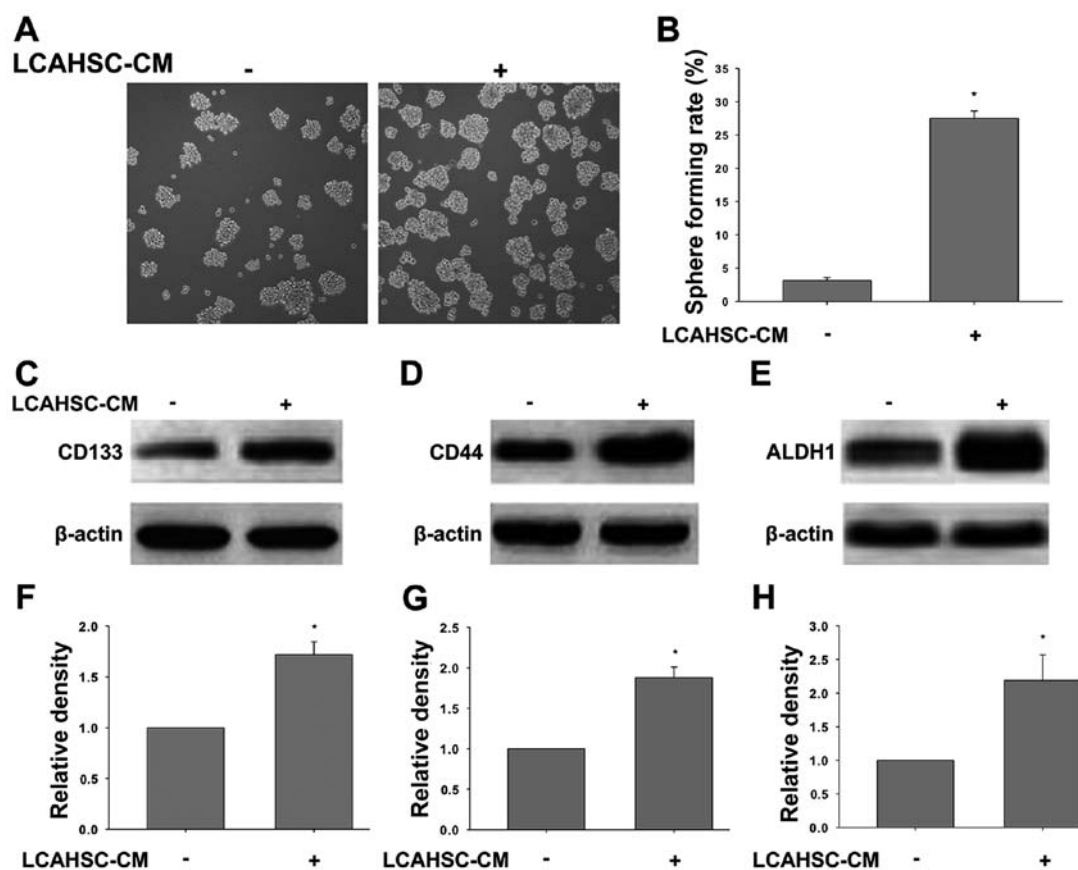


Figure 4. Increased expression of cancer stem cell markers and enhanced capability of sphere formation in SMMC-7721 cells treated with LCAHSC-CM. (A) Representative images of sphere forming cells from SMMC-7721 cells treated with (right) or without (left) LCAHSC-CM. (B) Sphere forming rate calculated by counting the number of sphere forming cells (* $P < 0.05$). Western blot of the expression of CD133 (C), CD44 (D) and ALDH1 (E) in SMMC-7721 cells treated with or without LCAHSC-CM. β -actin used as loading control. Densitometry analysis to quantify the expression of CD133 (F), CD44 (G) and ALDH1 (H) protein, respectively (* $P < 0.05$).

(LCAHSCs), and verify the capacity of LCSLC-CM-induce LX-2 cell pathologic activation. As shown in Fig. 2A, LX-2 cells treated with LCSLC-CM induced significant changes in fibroblast activation protein (FAP) expression, but no visible changes in α -smooth muscle actin (α -SMA) expression. This result is consistent with western blot analysis.

Effects of 8-bromo-7-methoxychrysin on activation of LX-2 cells by LCSLC-CM. We previously described that BrMC can inhibit several forms of cancer (31,33). In the current study, to analyze if BrMC can affect cross-talk of LCSLCs and HSCs to block the activation of HSC, we measured the expression of α -SMA and FAP by immunofluorescence and western blotting in LX-2 cells after being cultured with LCSLC-CM containing various concentrations of BrMC (0.0, 5.0, 10.0, 20.0 μ mol/l). As shown in Fig. 3A, immunofluorescence showed that BrMC had no effect on the expression of α -SMA, but it reduced the level of FAP expression in a dose-dependent manner. Consistent with the results of immunofluorescence, western blot analysis indicated downregulation of FAP (Fig. 3D and E), but not α -SMA (Fig. 3B and C).

Conditioned medium from liver cancer associated-stellate cells contributes to characteristics of LCSLCs derived from SMMC-7721 cells. To evaluate the effects of LCAHSCs on self-renewal capability and cancer stem cell marker expression

of SMMC-7721 cells and LCSLCs derived from SMMC-7721 cells, respectively; we collected conditioned medium from LCAHSCs (LCAHSC-CM), and the cells were exposed to LCAHSC-CM for 24 h. Then sphere formation assay and western blotting were performed. As expected, treatment with LCAHSC-CM enhanced the sphere forming ability of SMMC-7721 cells (Fig. 4A and B). The level of CD133 (Fig. 4C and F), CD44 (Fig. 4D and G) and ALDH1 (Fig. 4E and H) in the cells treated with LCAHSC-CM were significantly increased compared to untreated cells.

BrMC reverses the characteristics of LCSLCs induced by LCAHSC-CM. Our findings showed that LCAHSC-CM can promote the characteristics of LCSLCs and BrMC can inhibit activation of LX-2 cells. Thus, we investigated whether BrMC inhibits the characteristics of LCSLCs induced by LCAHSC-CM. Sphere forming assay indicated that BrMC inhibits self-renewal capability of SMMC-7721 cells in a dose-dependent manner, and the sphere forming rate was significant reduced when treatment with 20 μ mol/l BrMC (Fig. 5A and B). The markers of cancer stem cells (including CD133, CD44 and ALDH1) were also reduced by BrMC in a dose-dependent manner (Fig. 5C).

BrMC inhibits the phosphorylation of STAT3 in LX-2 cells induced by LCSLC-CM. It was reported that IL6/STAT3 axis

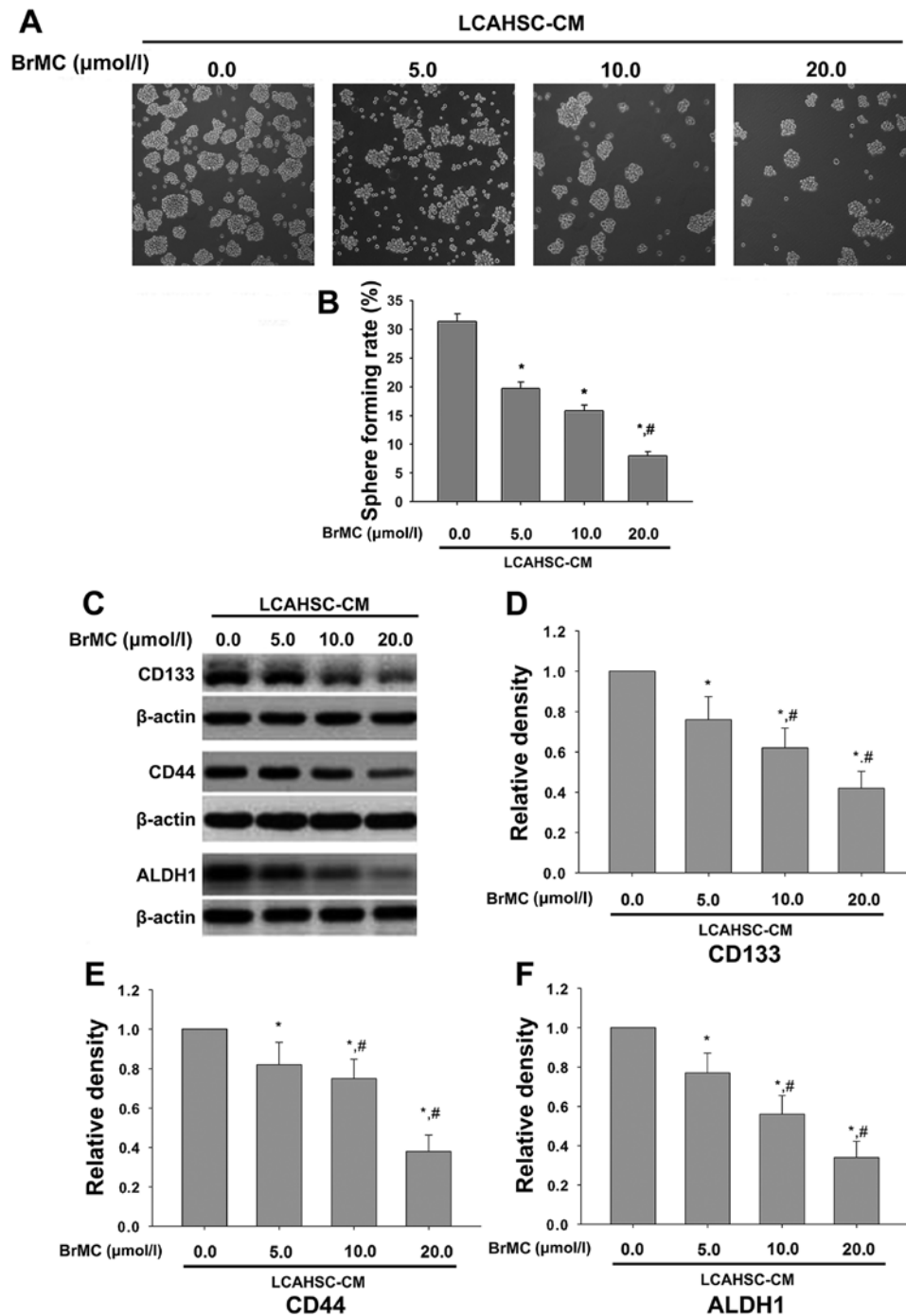


Figure 5. BrMC inhibits marker expression and sphere forming of LSCs induced by LCAHSC-CM. (A) Representative images of SMMC-7721 sphere forming induced by LCAHSC-CM when different concentrations of BrMC (0.0, 5.0, 10.0, 20.0 $\mu\text{mol/l}$) were added to LCAHSC-CM. (B) Calculating the number of sphere forming cells, and find the sphere forming rate was inhibited by BrMC in a dose-dependent manner (* $P < 0.05$). (C) Western blotting of the expression levels of CD133, CD44 and ALDH1, and β -actin was used as loading control. Densitometry analysis to quantify the expression of CD133 (D), CD44 (E) and ALDH1 (F) protein, respectively (* $P < 0.05$).

activated LX-2 cells (34). Thus, we studied whether STAT3 was responsible for LX-2 cells activation induced by LSC-CM, and if BrMC can decrease the phosphorylation of STAT3 to inhibit LX-2 cells activation. The results in Fig. 6A show that compared to serum-free DMEM/F12 medium, LSC-CM induced phosphorylation of STAT3 of LX-2 cells, but not total STAT3 protein expression. LSC-CM from LSCs treated with different concentrations of BrMC (0.0, 5.0, 10.0, 20.0 $\mu\text{mol/l}$), showed phosphorylation of STAT3 decreased in

a dose-dependent manner, and no effect on the level of STAT3 expression (Fig. 6B).

JSI-124 treatment reverses the characteristics of LSCs induced by LCAHSC-CM. The above studies showed that LSC-CM induced the phosphorylation of STAT3 in LX-2 cells and LCAHSC-CM contributed to the characteristics of LSCs. To explain the mechanism that activated the LX-2 cell promoted features of LSCs derived from SMMC-7721

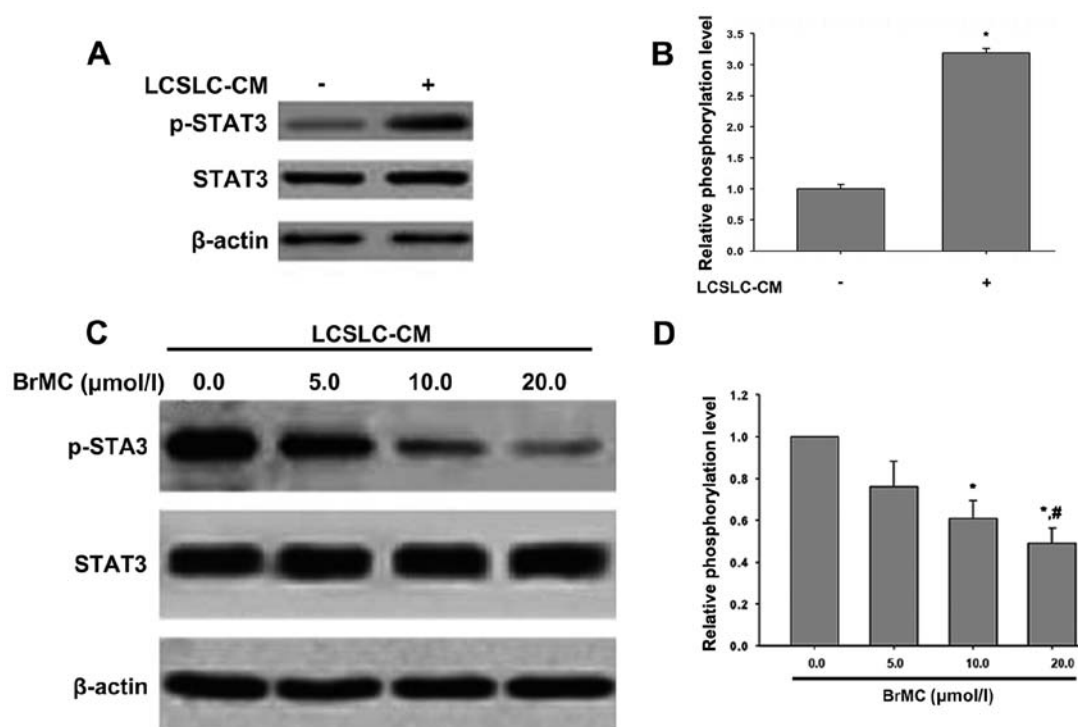


Figure 6. The phosphorylation of STAT3 in LX-2 cells induced by LCSLC-CM was inhibited by BrMC in a dose-dependent manner. (A and B) Cultured with or without LCSLC-CM, the phosphorylation of STAT3 in LX-2 cells had a significant difference ($P < 0.05$). (C and D) BrMC can reduce the phosphorylation of STAT3 in LX-2 cells induced by LCSLC-CM in a dose-dependent manner ($P < 0.05$).

cells, STAT3 inhibitor JSI-124 was used. Our findings showed that when added to LCSLC-CM treated with JSI-124, the phosphorylation of STAT3 in LX-2 cells was significantly reduced, but it had no effect on the expression of STAT3 compared with LCSLC-CM-treated LX-2 cells (Fig. 7A and B). Then we treated LCSLCs and SMMC-7721 cells with LCAHSC-CM containing different concentration of JSI-124 (0.0, 10.0, 30.0, 100.0 nmol/l) to determine their stem cell marker expression and sphere formation, respectively. Sphere formation induced by LCAHSC-CM was inhibited by JSI-124 in a dose-dependent manner (Fig. 7C). Western blotting showed that the level of cancer stem cell markers (CD133 (Fig. 7E), CD44 (Fig. 7G) and ALDH1 (Fig. 7I) were decreased after treated with JSI-124. In conclusion, JSI-124 inhibited the characteristics of LCSLCs induced by LCAHSC-CM.

BrMC and JSI-124 synergistically inhibit properties of LCSLCs induced by LCAHSC-CM. The above studies showed that BrMC reversed the characteristic of LCSLCs through inhibiting STAT3. Thus, we used STAT3 inhibitor JSI-124 (10 nmol/l) and BrMC (5.0 μ mol/l) alone or combined to administer LCSLCs and to obtain LCSLC-CM containing BrMC or JSI-124 or both, which was used to culture LX-2 cells for 24 h and collect LCAHSC-CM. Next, the STAT3 in LX-2 was determined by western blotting. We validated the role of BrMC and JSI-124 in the inhibition of the characteristics of LCSLCs. Our data showed that the presence of BrMC and JSI-124 was sufficient to reduce phosphorylation of STAT3, which indicated that BrMC and JSI-124 synergistically inhibited LX-2, which permitted them to be activated by LCSLC-CM (Fig. 8A). Then we collected LCAHSC-CM that contained BrMC and JSI-124 alone or combined to measure properties of LCSLCs.

The sphere forming assay showed that combined BrMC (5.0 μ mol/l) and JSI-124 (10 nmol/l) significantly inhibited the ability of sphere forming compared to treating with BrMC and JSI-124 alone (Fig. 8C). Then, western blotting was carried out to detect the expression of stem-cell markers (CD133, CD44 and ALDH1). The results indicated that combination of BrMC (5.0 μ mol/l) and JSI-124 (10 nmol/l) had a significant impact on the levels of CD133, CD44 and ALDH1 expression compared to BrMC or JSI-124 alone (Fig. 8E).

Discussion

LCSCs are considered the key factors of HCC progress. In addition, the tumor microenvironment plays an important role during carcinogenesis. Carcinoma-associated fibroblasts (CAFs) are one of the most crucial components of the HCC microenvironment. In this study, we put forward that human hepatic stellate cell line LX-2 can be activated to a myofibroblast-like phenotype through STAT3 pathway, and activated LX-2 cells in turn promote the characteristics of LCSLCs. Moreover, BrMC affected cross-talk of LCSLCs and LX-2 cells to reduce the activation of HSC and then reversed the characteristics of LCSLCs.

CAFs are thought to be activated, which is characterized by the expression of α -SMA and FAP (35-37). Moreover, activated fibroblasts in tumor tissues are considered as CAFs. In our present study, we proved that LCSLCs derived from SMMC-7721 cells had interaction with LX-2 cells, and made LX-2 cells pathologically activated with a myofibroblast-like phenotype, named LCAHSC. Our results are consistent with the identification of activated CAFs as these cells expressed α -SMA and FAP, whereas cells treated without LCSLC-CM

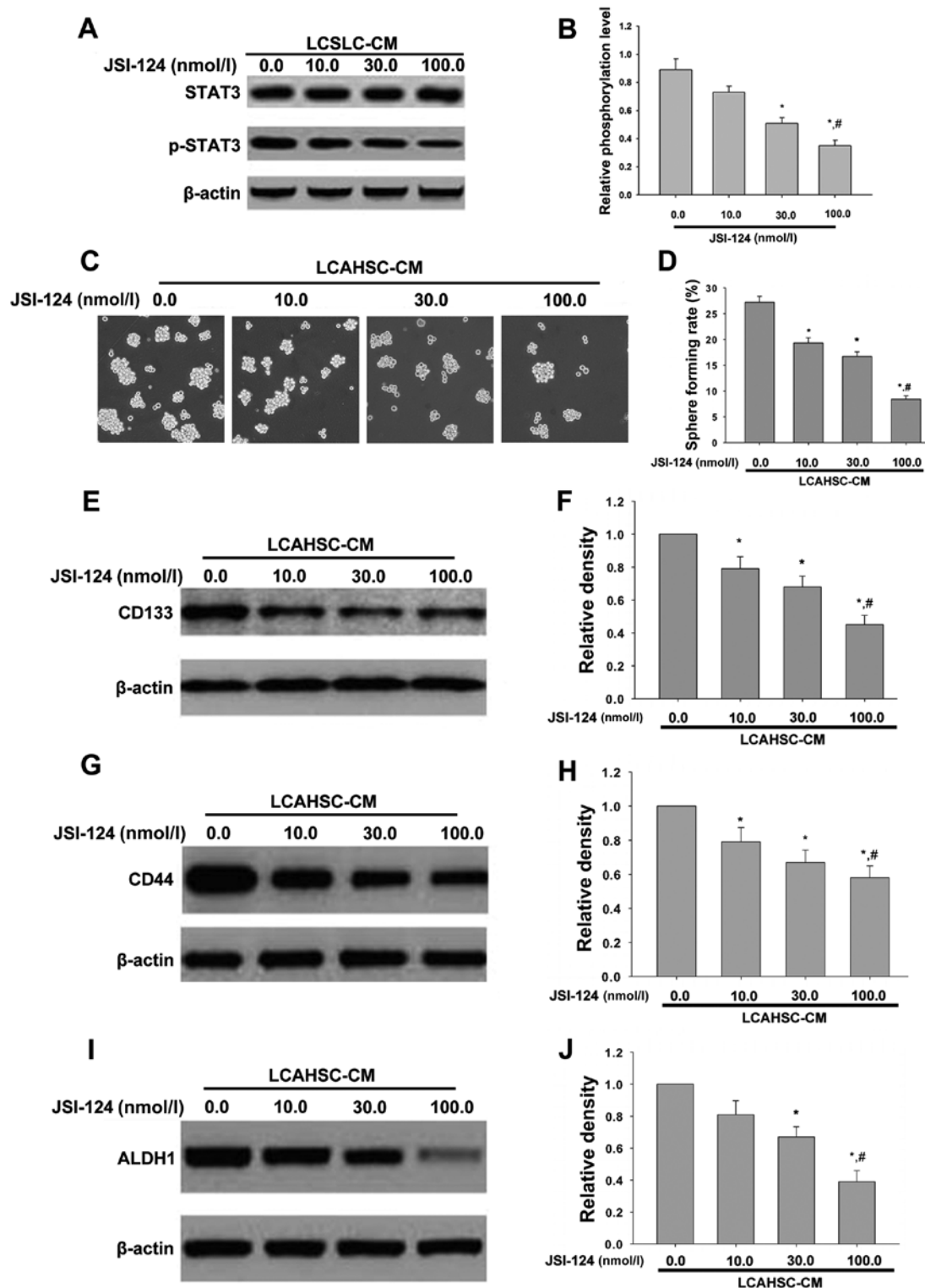


Figure 7. JSI-124 inhibits STAT3 activation in LX-2 cells and sphere formation and marker expression of SMMC-7721 cells induced by LCSLC-CM. (A) After being culturing with JSI-124, the phosphorylation of STAT3 induced by LCSLC-CM in LX-2 cells was significantly reduced. (B) Densitometry analysis to quantify the expression of p-STAT3 (* P <0.05). (C) Sphere forming of LCSLCs treated with LCAHSC-CM containing JSI-124. (D) Sphere forming rate determined by counting number of sphere forming cells (* P <0.05). Expression of stem cell markers CD133 (E), CD44 (G), and ALDH1 (I) in LCSLCs. Densitometry analysis to quantify the expression of CD133 (F), CD44 (H), and ALDH1 (J) (* P <0.05).

did not express FAP (Fig. 2). Noteworthy, the LX-2 cells treated without LCSLC-CM also express α -SMA, which suggests that these cells exist in an activated state under cell culture conditions. We found that the conditioned medium from pathologically activated LX-2 cells significantly

promoted the characteristics of LCSLCs of the SMMC-7721 cell line (Fig. 3).

STAT3, a transcription factor mediating various cellular processes and participating in cellular transformation, is aberrantly activated in numerous cancer types, including

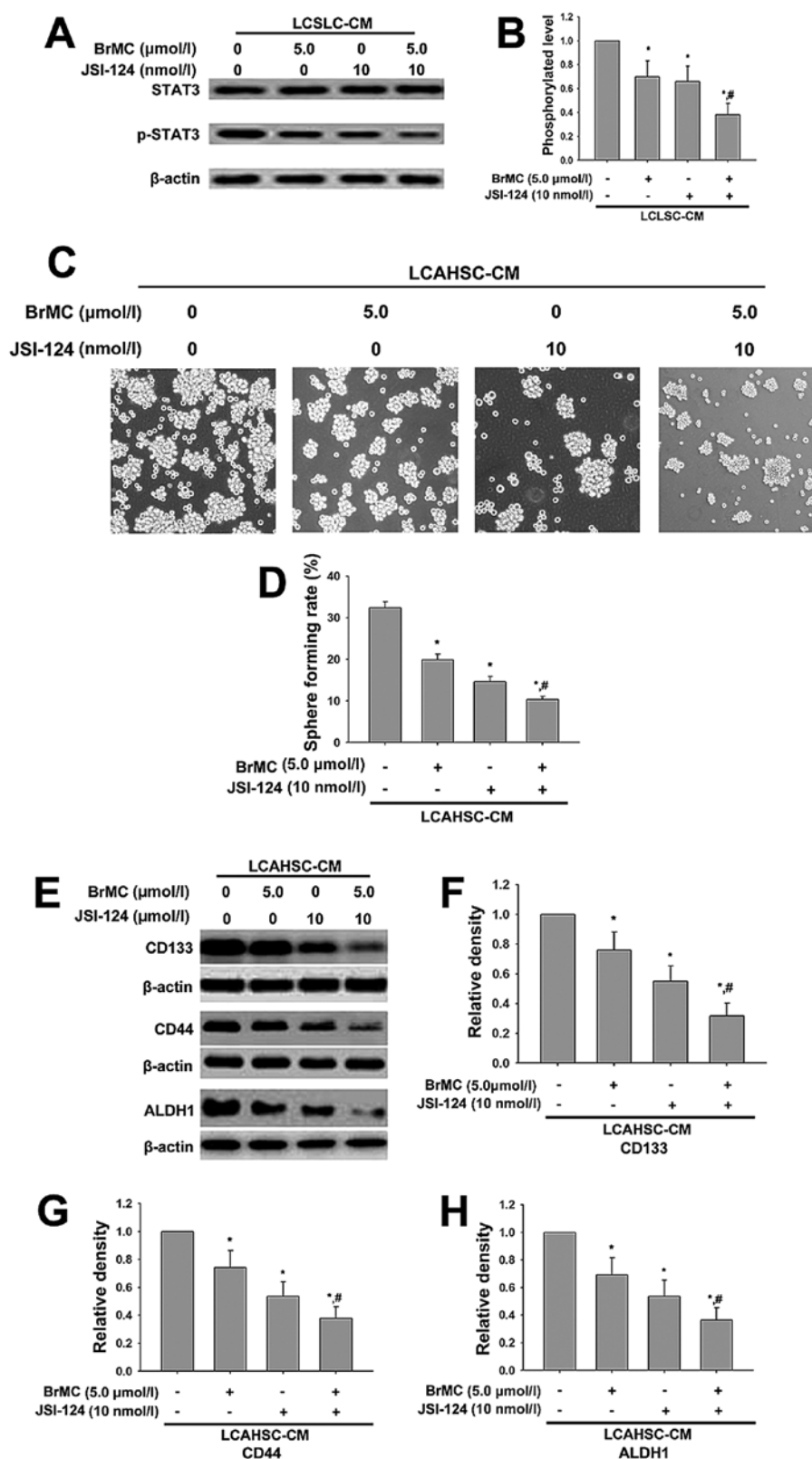


Figure 8. BrMC and JSI-124 synergistically inhibit sphere forming and stem-cell marker expression of LCSLCs, as well as the activation of STAT3 in LCAHSC. (A) Combined administration of BrMC (1 $\mu\text{mol/l}$) and JSI-124 (10 nmol/l) and the relative expression level of p-STAT3 in LX-2 cells. (B) Densitometry quantification of both p-STAT3 and STAT3 expression ($P < 0.05$). (C) Representative images of sphere forming of LCSLCs cultured with LCAHSC-CM which contains BrMC (5.0 $\mu\text{mol/l}$) and JSI-124 (10 nmol/l). (D) Calculation of the sphere forming cells, and the bar graph ($P < 0.05$). (E) Western blot expression of CD133, CD44 and ALDH1 in LCSLCs. Densitometry analysis to quantify the expression of CD133 (F), CD44 (G) and ALDH1 (H) ($P < 0.05$).

HCC. Since the persistent activation of STAT3 promotes tumor cell proliferation and survival, contributing to tumor

progression, abrogation of STAT3 signaling is emerging as a potential cancer therapy strategy (38). We found that the level

of p-STAT3 was greater in LX-2 cell treated with LCSLC-CM than control (Fig. 6A). JSI-124, an inhibitor of the JAK/STAT pathway, could effectively block STAT3 signaling in a dose-dependent manner, and further inhibited the characteristics of liver cancer stem-like cells induced by LCAHSC-CM (Fig. 7). To our knowledge, this is the first study to demonstrate that the STAT3 plays an important role in the interaction of LCSLCs and LX-2 cells.

8-bromo-7-methoxychrysin (BrMC) was synthesized previously based of the lead compound ChR (28). In addition, BrMC has strong effects of inhibition of proliferation and induction of apoptosis on various types of cancer (39,40). In the current study, we demonstrated that BrMC significantly reduced the activation of LX-2 induced by LCSLC-CM, and inhibited the properties of LCSLCs induced by LCAHSC-CM (Fig. 4). Of note, the level of p-STAT3 in LCAHSC was greatly decreased after treated with BrMC (Fig. 6C), suggesting BrMC could inhibit the activation of LX-2 induced by LCSLC-CM through attenuating STAT3 activation, and then reversed the characteristics of LCSLCs induced by LCAHSC-CM.

Our data also showed that BrMC (5.0 μ mol/l) and JSI-124 (10 nmol/l) synergistically inhibited the expression of p-STAT3 in LX-2 cells, and the expression levels of α -SMA and FAP decreased in response to BrMC (5.0 μ mol/l) and JSI-124 (10 nmol/l), which support the possibility that inhibition of the STAT3 pathway may significantly block transformation of LX-2 cells from a quiescent state into a myofibroblast-like phenotype. Then, combination of BrMC (5.0 μ mol/l) and JSI-124 (10 nmol/l) significantly decreased the sphere formation and the expression levels of stem cell markers (CD133, CD44 and ALDH1) (Fig. 8). Taken together, our findings indicated that combined BrMC and JSI-124 significantly inhibited cross-talk of LX-2 cells and LCSLCs probably through suppressing the activation of STAT3.

Compared with LCSCs, the relevance between LCSCs, hepatic stellate cells, and STAT3 have been less clearly identified. A recent report demonstrated that IL6/STAT3 axis was sufficient for transdifferentiation of quiescent fibroblasts to CAFs (34). It was reported that cross-talk between hepatoma cells and activated HSCs engendered a permissive inflammatory microenvironment that drives HCC progression (12). In this study, we discovered that human hepatic stellate cell line LX-2 could be activated by LCSLC-CM through STAT3 signaling pathway, which was inhibited by BrMC. However, the establishment of co-culture model may be required to further demonstrate the physiological significance of cross-talk of LCSLCs and LX-2 cells. Additionally, LCSLCs-HSC cross-talk may result in extracellular matrix remodeling, which can be associated with STAT3 signaling pathway. Studies might also be necessary to explain the change of cytokine composing extracellular matrix.

In conclusion, we demonstrated that the STAT3 signaling may be responsible for the interaction of LX-2 cells and LCSLCs. BrMC and JSI-124 synergistically attenuate the CSC-like properties induced by LCAHSC-CM through inhibiting STAT3 activation and may present a potential clinical benefit for the treatment of HCC. Thus, there is a great need to unravel the underlying mechanisms of the STAT3 pathway in cross-talk of LX-2 cells and LCSLCs and

to further evaluate the therapeutic possibilities of combination with JSI-124 and BrMC.

Acknowledgements

This study was supported by a Project of the NSFC (grant nos. 30760248, 31400311 and 81172375), the Project of Scientific Research Fund of Hunan Provincial Education Department (grant no. 14C0707), the Project of Hunan Provincial Natural Science Foundation (grant no. 13JJ3061) and the Scientific Research Fund of Hunan Normal University (grant nos. 140668 and 140666).

References

1. Dudeck O and Ricke J: Advances in regional chemotherapy of the liver. *Expert Opin Drug Deliv* 8: 1057-1069, 2011.
2. Torre LA, Bray F, Siegel RL, Ferlay J, Lortet-Tieulent J and Jemal A: Global cancer statistics, 2012. *CA Cancer J Clin* 65: 87-108, 2015.
3. Oishi N and Wang XW: Novel therapeutic strategies for targeting liver cancer stem cells. *Int J Biol Sci* 7: 517-535, 2011.
4. Ma S, Chan KW, Lee TK, Tang KH, Wo JY, Zheng BJ and Guan XY: Aldehyde dehydrogenase discriminates the CD133 liver cancer stem cell populations. *Mol Cancer Res* 6: 1146-1153, 2008.
5. Huang X, Sheng Y and Guan M: Co-expression of stem cell genes CD133 and CD44 in colorectal cancers with early liver metastasis. *Surg Oncol* 21: 103-107, 2012.
6. Zhang H, Chang WJ, Li XY, Zhang N, Kong JJ and Wang YF: Liver cancer stem cells are selectively enriched by low-dose cisplatin. *Braz J Med Biol Res* 47: 478-482, 2014.
7. Faurobert E, Bouin AP and Albiges-Rizo C: Microenvironment, tumor cell plasticity, and cancer. *Curr Opin Oncol* 27: 64-70, 2015.
8. Ye J, Wu D, Wu P, Chen Z and Huang J: The cancer stem cell niche: Cross talk between cancer stem cells and their micro-environment. *Tumour Biol* 35: 3945-3951, 2014.
9. Wang BB, Cheng JY, Gao HH, Zhang Y, Chen ZN and Bian H: Hepatic stellate cells in inflammation-fibrosis-carcinoma axis. *Anat Rec (Hoboken)* 293: 1492-1496, 2010.
10. Friedman SL: Hepatic stellate cells: Protean, multifunctional, and enigmatic cells of the liver. *Physiol Rev* 88: 125-172, 2008.
11. Friedman SL, Sheppard D, Duffield JS and Violette S: Therapy for fibrotic diseases: Nearing the starting line. *Sci Transl Med* 5: 167sr1, 2013.
12. Coulouarn C, Corlu A, Glaire D, Guénon I, Thorgeirsson SS and Clément B: Hepatocyte-stellate cell cross-talk in the liver engenders a permissive inflammatory microenvironment that drives progression in hepatocellular carcinoma. *Cancer Res* 72: 2533-2542, 2012.
13. Jia CC, Wang TT, Liu W, Fu BS, Hua X, Wang GY, Li TJ, Li X, Wu XY, Tai Y, *et al*: Cancer-associated fibroblasts from hepatocellular carcinoma promote malignant cell proliferation by HGF secretion. *PLoS One* 8: e63243, 2013.
14. Han Z, Wang X, Ma L, Chen L, Xiao M, Huang L, Cao Y, Bai J, Ma D, Zhou J, *et al*: Inhibition of STAT3 signaling targets both tumor-initiating and differentiated cell populations in prostate cancer. *Oncotarget* 5: 8416-8428, 2014.
15. Bharadwaj U, Eckols TK, Kolosov M, Kasembeli MM, Adam A, Torres D, Zhang X, Dobrolecki LE, Wei W, Lewis MT, *et al*: Drug-repositioning screening identified piperlongumine as a direct STAT3 inhibitor with potent activity against breast cancer. *Oncogene* 34: 1341-1353, 2015.
16. Liu C, Zeng Y, Dai LH, Cai TY, Zhu YM, Dou DQ, Ma LQ and Sun YX: Mogrol represents a novel leukemia therapeutic, via ERK and STAT3 inhibition. *Am J Cancer Res* 5: 1308-1318, 2015.
17. Stechshin OD, Luchman HA, Ruan Y, Blough MD, Nguyen SA, Kelly JJ, Cairncross JG and Weiss S: On-target JAK2/STAT3 inhibition slows disease progression in orthotopic xenografts of human glioblastoma brain tumor stem cells. *Neuro Oncol* 15: 198-207, 2013.

18. Song L, Rawal B, Nemeth JA and Haura EB: JAK1 activates STAT3 activity in non-small-cell lung cancer cells and IL-6 neutralizing antibodies can suppress JAK1-STAT3 signaling. *Mol Cancer Ther* 10: 481-494, 2011.
19. Niu G, Wright KL, Ma Y, Wright GM, Huang M, Irby R, Briggs J, Karras J, Cress WD, Pardoll D, *et al*: Role of Stat3 in regulating p53 expression and function. *Mol Cell Biol* 25: 7432-7440, 2005.
20. Wan S, Zhao E, Kryczek I, Vatan L, Sadovskaya A, Ludema G, Simeone DM, Zou W and Welling TH: Tumor-associated macrophages produce interleukin 6 and signal via STAT3 to promote expansion of human hepatocellular carcinoma stem cells. *Gastroenterology* 147: 1393-1404, 2014.
21. Nieto N: Oxidative-stress and IL-6 mediate the fibrogenic effects of [corrected] Kupffer cells on stellate cells. *Hepatology* 44: 1487-1501, 2006.
22. Handy JA, Saxena NK, Fu P, Lin S, Mells JE, Gupta NA and Anania FA: Adiponectin activation of AMPK disrupts leptin-mediated hepatic fibrosis via suppressors of cytokine signaling (SOCS-3). *J Cell Biochem* 110: 1195-1207, 2010.
23. Qi J, Xia G, Huang CR, Wang JX and Zhang J: JSI-124 (Cucurbitacin I) inhibits tumor angiogenesis of human breast cancer through reduction of STAT3 phosphorylation. *Am J Chin Med* 43: 337-347, 2015.
24. Brechbuhl HM, Kachadourian R, Min E, Chan D and Day BJ: Chrysin enhances doxorubicin-induced cytotoxicity in human lung epithelial cancer cell lines: The role of glutathione. *Toxicol Appl Pharmacol* 258: 1-9, 2012.
25. Sun X, Huo X, Luo T, Li M, Yin Y and Jiang Y: The anticancer flavonoid chrysin induces the unfolded protein response in hepatoma cells. *J Cell Mol Med* 15: 2389-2398, 2011.
26. Lirdprapamongkol K, Sakurai H, Abdelhamed S, Yokoyama S, Athikomkulchai S, Viriyaraj A, Awale S, Ruchirawat S, Svasti J and Saiki I: Chrysin overcomes TRAIL resistance of cancer cells through Mcl-1 downregulation by inhibiting STAT3 phosphorylation. *Int J Oncol* 43: 329-337, 2013.
27. Lin CM, Shyu KG, Wang BW, Chang H, Chen YH and Chiu JH: Chrysin suppresses IL-6-induced angiogenesis via down-regulation of JAK1/STAT3 and VEGF: An in vitro and in ovo approach. *J Agric Food Chem* 58: 7082-7087, 2010.
28. Zheng X, Meng WD, Xu YY, Cao JG and Qing FL: Synthesis and anticancer effect of chrysin derivatives. *Bioorg Med Chem Lett* 13: 881-884, 2003.
29. Ai XH, Zheng X, Tang XQ, Sun L, Zhang YQ, Qin Y, Liu HQ, Xia H and Cao JG: Induction of apoptosis of human gastric carcinoma SGC-7901 cell line by 5, 7-dihydroxy-8-nitrochrysin in vitro. *World J Gastroenterol* 13: 3824-3828, 2007.
30. Ren KQ, Cao XZ, Liu ZH, Guo H, Quan MF, Liu F, Jiang L, Xiang HL, Deng XY and Cao JG: 8-bromo-5-hydroxy-7-methoxychrysin targeting for inhibition of the properties of liver cancer stem cells by modulation of Twist signaling. *Int J Oncol* 43: 1719-1729, 2013.
31. Quan MF, Xiao LH, Liu ZH, Guo H, Ren KQ, Liu F, Cao JG and Deng XY: 8-bromo-7-methoxychrysin inhibits properties of liver cancer stem cells via downregulation of β -catenin. *World J Gastroenterol* 19: 7680-7695, 2013.
32. Ning Y, Li Q, Xiang H, Liu F and Cao J: Apoptosis induced by 7-difluoromethoxyl-5,4'-di-n-octyl genistein via the inactivation of FoxM1 in ovarian cancer cells. *Oncol Rep* 27: 1857-1864, 2012.
33. Cao XZ, Xiang HL, Quan MF and He LH: Inhibition of cell growth by BrMC through inactivation of Akt in HER-2/neu-overexpressing breast cancer cells. *Oncol Lett* 7: 1632-1638, 2014.
34. Lee KW, Yeo SY, Sung CO and Kim SH: Twist1 is a key regulator of cancer-associated fibroblasts. *Cancer Res* 75: 73-85, 2015.
35. Kalluri R and Zeisberg M: Fibroblasts in cancer. *Nat Rev Cancer* 6: 392-401, 2006.
36. Pietras K and Ostman A: Hallmarks of cancer: Interactions with the tumor stroma. *Exp Cell Res* 316: 1324-1331, 2010.
37. Xing F, Saidou J and Watabe K: Cancer associated fibroblasts (CAFs) in tumor microenvironment. *Front Biosci (Landmark Ed)* 15: 166-179, 2010.
38. Yu H and Jove R: The STATs of cancer - new molecular targets come of age. *Nat Rev Cancer* 4: 97-105, 2004.
39. Yang XH, Zheng X, Cao JG, Xiang HL, Liu F and Lv Y: 8-Bromo-7-methoxychrysin-induced apoptosis of hepatocellular carcinoma cells involves ROS and JNK. *World J Gastroenterol* 16: 3385-3393, 2010.
40. Xiao G, Tang X, Yao C and Wang C: Potentiation of arsenic trioxide-induced apoptosis by 8-bromo-7-methoxychrysin in human leukemia cells involves depletion of intracellular reduced glutathione. *Acta Biochim Biophys Sin (Shanghai)* 43: 712-721, 2011.